Available online at www.sciencedirect.com
SCIENCE DIRECT®
International Journal of Heat and Mass Transfer 47 (2004) 407–411
International Journal of HEAT and MASS TRANSFER
www.elsevier.com/locate/ijhmt

Technical Note

Pool boiling heat transfer experiments in silica–water nano-fluids

Peter Vassallo [a,*], Ranganathan Kumar [b], Stephen D'Amico [a]

[a] Lockheed Martin Corporation, Schenectady, NY 12301, USA
[b] Department of Mechanical, Materials and Aerospace Engineering, University of Central Florida, Orlando, FL 32816, USA

Received 31 March 2003; received in revised form 2 July 2003

Abstract

Heat transfer measurements taken at atmospheric pressure in silica nano-solutions are compared to similar measurements taken in pure water and silica micro-solutions. The data include heat flux vs. superheat of a 0.4 mm diameter NiCr wire submerged in each solution. The data show a marked increase in critical heat flux (CHF) for both nano- and micro-solutions compared to water, but no appreciable differences in heat transfer for powers less than CHF. The data also show that stable film boiling at temperatures close to the wire melting point are achievable with the nano-solutions but not with the micro-solutions.

1. Introduction

Considerable research is currently underway to understand the heat transfer behavior of nano-solutions, or solutions obtained by adding small concentrations of nano-meter sized particles to liquids [1–3]. One area of interest is in boiling flow systems, where the ability to enhance heat transfer would improve the overall efficiency of the systems, reduce operational cost and provide greater safety margins if the maximum heat flux limit could be increased. The effect of nano-particles on heat transfer is currently hard to predict; in one recent study [4], the heat transfer in a pool boiling system actually decreased with the addition of Al_2O_3 particles. In this work, the pool boiling behavior of silica particles with diameters ranging from 15 to 3000 nm is studied, and boiling curves are generated from the nucleate boiling to the film boiling regimes under atmospheric pressure.

2. Description of experiment

The experiments were conducted by passing current through the NiCr wire horizontally suspended in saturated deionized water at atmospheric pressure. The NiCr wire (~75 mm length) was soldered to 18 gage copper lead wires and held tightly underwater using threaded rod attached to a steel cover. A Pyrex dish contained the water (~300 ml); the wire was fully wetted and no effect on the data was observed as the water level decreased from ~12 mm above the wire to ~6 mm as the experiments progressed. A Kenwood power supply (20 A capacity) operating in constant current mode provided the power and calibrated Keithley and Hewlett–Packard multi-meters were used to measure the current and voltage to within 1 mA and 1 mV respectively. The water was heated to boiling within the Pyrex dish using a Thermolyne hot plate and the bulk boiling temperature was measured with a type-K thermocouple.

In taking the data, the system resistance was first measured through the power supply, meters and lead wires by connecting the lead wires together and measuring the voltage at low power (<1 A). This system resistance was subtracted later from the resistance measurements obtained with the NiCr wire attached to

* Corresponding author. Tel.: +1-518-395-6799; fax: +1-518-395-5353.
E-mail address: vassall@kapl.gov (P. Vassallo).

0017-9310/$ - see front matter © 2003 Elsevier Ltd. All rights reserved.
doi:10.1016/S0017-9310(03)00361-2

the lead wires. The system resistance was between 0.08 and 0.11 Ω, depending on the length of the lead wires. A baseline measurement of the NiCr wire resistance was taken at the beginning of each data run in boiling water at 100 °C. This resistance (typically 0.6–0.7 Ω) was calculated from:

$$R_W = \frac{V}{I} - R_S \tag{1}$$

where R_W = NiCr wire resistance, V = measured voltage, I = measured current (<1 A) and R_S = system resistance excluding NiCr wire. The system was cycled several times by applying upwards of 10 A to the wire (significant boiling) and returning to ~1 A (no boiling) to confirm the repeatability of the baseline value to within ±0.001 Ω. The boiling curve data were then taken by slowly increasing the current and recording the current and voltage readings at each point. Note: boiling was initiated at a few isolated spots on the wire when the current was ~2.5 A. If the wire was taken to failure, at some current level (>12 A) the wire would either suddenly break or become red and subsequently break as the current was increased. If measurements in particulate solutions were desired, some limited data (<10 A) were usually taken in water to confirm the expected response of the wire, then the water was replaced by the solution with no other changes being made. This improved the reliability of subsequent comparisons between the pure water boiling curve and the boiling curve in the particulate solutions.

The boiling curves were generated by deriving the wire temperature from a known temperature–resistance relationship and obtaining the heat flux from the measured current and resistance. The temperature–resistance curve was obtained for NiCr from technical data summarized by Hyndman [5]. This curve did not go all the way to the melting point (terminated at 1200 °C) so the curve was extended to the melting temperature (1400 °C) by including the present burn-out data. The temperature–resistance relationship has the form:

$$\frac{T}{T_{base}} = f\left(\frac{R}{R_{base}}\right) \tag{2}$$

Eq. (2) indicates that it is more important to know the percent increase in wire resistance relative to the baseline value (in this case, $T = 100$ °C) than it is to know the absolute value of the resistance. In this way, any constant bias in the measurements is effectively removed.

The heat flux was obtained from:

$$q'' = \frac{I^2 R_W}{\pi D L} \tag{3}$$

where R_W is given by Eq. (1), D is the wire diameter and L is the wire length.

3. Results and discussion

3.1. Pure water data

The boiling curve data taken in pure water are summarized in Fig. 1. The wire superheat is defined as ($T_W - 100$ °C) [1] and the heat flux is defined as in Eq. (3). The typical regions of pool boiling first described by investigators such as Nukiyama [6] and Jakob and Linke [7] are observed here as well. At low superheats (i.e., <10 °C) the natural convection regime is observed where no boiling occurs, then a sharp rise in heat flux is evident as nucleation begins. The nucleate boiling regime continues until the maximum heat flux is reached whereupon the vapor blankets the wire and the temperature suddenly rises as transition occurs into the film boiling regime. The wire usually breaks, or melts, at the location of maximum flux (also called critical heat flux, or CHF) or shortly after entering the film boiling regime. The bold data points in Fig. 1 indicate data sets that were taken to failure while the remaining points indicate data sets limited to lower powers.

The Zuber correlation for CHF [8] is given as:

$$q''_{max} = 0.131 h_{fg} \rho_v^{1/2} (g\sigma\Delta\rho)^{1/4} \tag{4}$$

This correlation is included in Fig. 1 and predicts the data well. For most of the data sets, the wire fails close to this critical heat flux. In one data set, the wire was observed to fail at ~25% higher than the others at $\Delta T = 60$ °C. This is believed to be due to some different surface characteristics for that particular wire that would affect its nucleation site density and lead to its ability to sustain higher heat fluxes. This effect, and the scratched wire data in Fig. 1, will be discussed more later. In general, though, most new wires fail within 10% of the Zuber prediction, and this can be used as the basis for subsequent CHF comparisons.

The nucleate boiling expressions in Refs. [9,10], applicable for larger diameter horizontal cylinders, and in Refs. [10,11], applicable for small cylinders (and here evaluated at $D = 0.4$ mm) are also included in Fig. 1. Both expressions adequately bound the present data. The surface characteristics of the wire will affect the boiling curve somewhat (demonstrated by the shift in the curve for the scratched wires in Fig. 1) and may explain some of the deviations between the data and prediction. The important things to note in Fig. 1, for later comparisons with nano-solution data, is the scatter in the data and the trend indicated by the data curve fit.

[1] This is a nominal value of the water boiling temperature, corresponding to $P = 1.0133$ bars. The uncertainty in water boiling temperature is estimated as ±0.4 °C, which reflects the small day to day variations in atmospheric pressure experienced within the test environment.

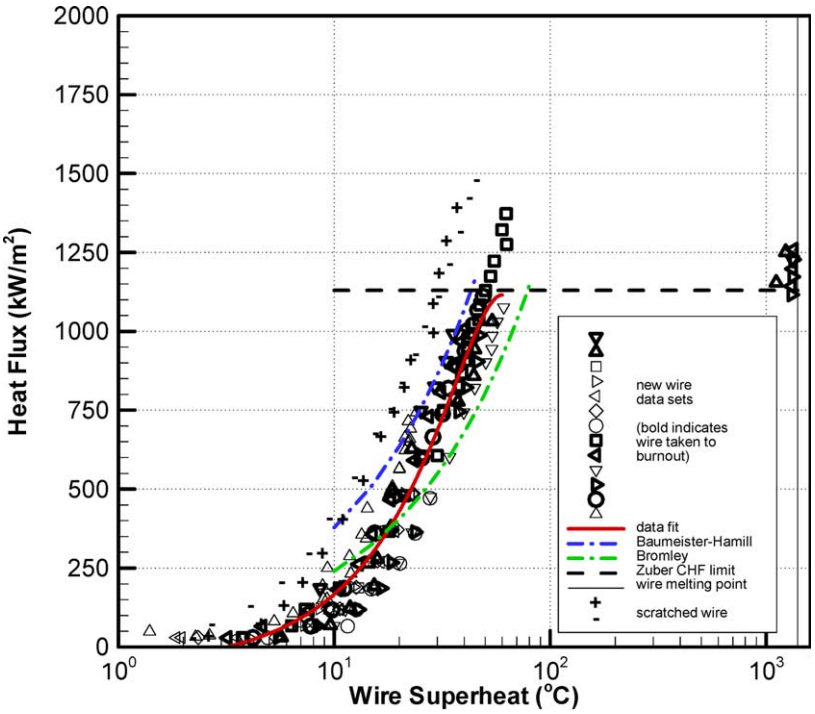

Fig. 1. Boiling curves of NiCr wire ($D = 0.4$ mm) in pure water.

The data scatter is mainly due to the uncertainty in the temperature calculation. Based on a resistance uncertainty relative to baseline of ±0.15%, the uncertainty in temperature calculation is ±8.2 °C at a given heat flux. The uncertainty in heat flux is mainly attributed to the uncertainty in the wire diameter and length. The heat flux uncertainty is estimated to be ±2%.

3.2. Silica particle data

The silica nano-solutions were studied first. Both nano-solutions were obtained from Cornell University; they included nominal 15 and 50 nm diameter particles at volume concentrations between 2% and 9% (water being the solvent). The final concentration used in these tests was 0.5% by volume, obtained by mixing the appropriate amounts of deionized water and nano-solution together. This is a nominal value and may have changed somewhat during the experiments as evaporation occurred (about 25% of the water was evaporated by the end of the tests). However, even if all the particles remained in solution (i.e., none was carried away by the vapor) the particle concentration at the end of the test would have only increased from 0.5% to 0.67%; this is not believed to significantly affect the results described or conclusions drawn.

All of the data for the silica particles is shown in Fig. 2. Also shown is the curve fit for the pure water boiling data. Within the scatter of the data, the boiling curves for both 15 and 50 nm particles follow the pure water boiling curve throughout the nucleate boiling regime up to the CHF limit, then continue significantly higher (i.e., ~60% higher) before transitioning into the film boiling regime. There does not appear to be any heat transfer enhancement in the nucleate boiling regime, but the CHF limit is clearly increased for the nano-particles. [2] For two of the data sets using 15 nm particles, the wire failed transitioning into film boiling, while for the third data set, the wire failed well into the film boiling regime. The wire glowed a bright red for the last ten data points before breaking. A similar trend was observed for the 50 nm particles, with an even greater increase in sustainable heat flux. The wire never failed in the 50 nm solution and was able to sustain the maximum current for the power supply (20 A). It is noted that a silica coating (0.15–0.2 mm) was observed on the wire at the end of testing, indicating some possible surface interaction with the wire at higher heat fluxes.

To examine the system response to larger silica particles, a 0.5% volume solution of 3 μm silica particles

[2] Although some of the silica boiling curves appear higher than the mean pure water curve fit, the particular baseline water points are close to their corresponding silica points and, at best, indicate a minor enhancement for heat fluxes less than CHF.

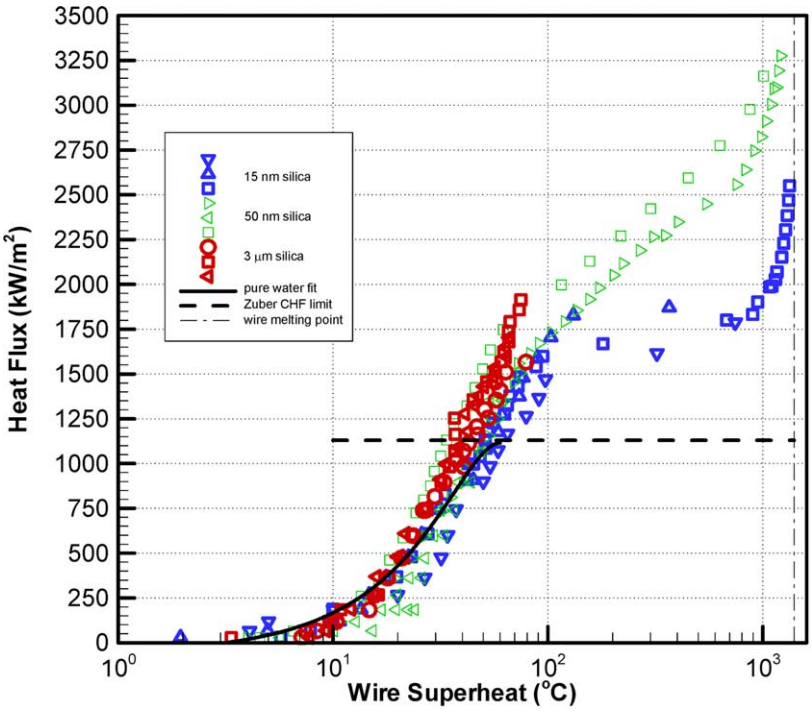

Fig. 2. Boiling curves of NiCr wire ($D = 0.4$ mm) in silica–water solutions.

was also tested. Remarkably, the larger silica particles again dramatically increased the CHF point, with no significant improvement observed at lower powers. One large distinction between the 3 μm silica particles and the nano-particles is that the wire always failed prior to entering the film boiling regime for the larger particles. Another distinction is that many of the larger 3 μm particles quickly settled out in the bottom of the Pyrex dish while the nano-particles remained more dispersed. This limits the overall attractiveness of micron sized particles in a flowing system where fouling is a concern. At the end of the tests, a thin silica coating (0.025–0.05 mm) was observed on the wire.

The coating of the silica suggests a possible surface roughness effect that would change the nucleation site density and improve the heat transfer [12]. To test this, wires were artificially roughened with emery paper and tested in pure water. The results are shown in Fig. 1. Indeed, the increased roughness led to a higher attainable heat flux at a given wire superheat within the nucleate boiling regime and even a higher CHF point than the virgin wire. However, it does not appear that this alone would explain the dramatic heat-fluxes attained with the nano-solutions nor, for that matter, with the 3 μm silica solution. More work is needed to fully understand the mechanisms responsible for these large gains in heat transfer at high heat flux. One thing is clear: the addition of nano-particles vs. micron sized particles allows a significant increase in heat transfer at high heat flux and leads to sustainable operation within the film boiling regime at temperatures close to the melting point. The 50 nm silica solution allows a maximum heat flux about 3 times that of pure water and nearly twice that allowed with the 3 μm silica solution.

Acknowledgements

The authors acknowledge the contributions of Dr. Ulrich Weisner from Cornell University for his preparation of the nano-solutions and Christopher Regan and Charles Zarnofsky for their help in setting up the experiment.

References

[1] J.A. Eastman, U.S. Choi, S. Li, Development of energy-efficient nanofluids for heat transfer applications, Research Briefs Argonne National Laboratory, 2000.
[2] Y. Xuan, Q. Li, Heat transfer enhancements of nanofluids, Int. J. Heat Fluid Flow 21 (2000) 58–64.
[3] Y. Xuan, W. Roetzel, Conceptions for heat correlation of nanofluids, Int. J. Heat Mass Transfer 43 (2000) 3701–3707.
[4] S.K. Das, N. Putra, W. Roetzel, Pool boiling characteristics of nano-fluids, Int. J. Heat Mass Transfer 46 (2003) 851–862.

[5] Hyndman Industrial Products, Inc., Resistance wire heating data, www.resistancewire.com, 2003.
[6] S. Nukiyama, The maximum and minimum values of heat Q transmitted from metal to boiling water under atmospheric pressure, J. Jpn. Soc. Mech. Eng. 37 (1934) 367–374 (translated in Int. J. Heat Mass Transfer 9 (1966) 1419–1433).
[7] M. Jakob, W. Linke, Phys. Z. 36 (1935) 267.
[8] N. Zuber, Hydrodynamic aspects of boiling heat transfer, AEC Rep. AECU-4439, 1959.
[9] L.A. Bromley, Heat transfer in stable film boiling, Chem. Eng. Prog. 46 (5) (1950) 221–227.
[10] N. Bakhru, J.H. Lienhard, Boiling from small cylinders, Int. J. Heat Mass Transfer 15 (1972) 2011–2025.
[11] K.J. Baumeister, T.D. Hamill, Film boiling from a thin wire as an optimal boundary-value process, ASME Paper No. 67-HT-62, 1967.
[12] C. Corty, A.S. Foust, Surface variables in nucleate boiling, Chem. Eng. Prog. Symp. Ser. 17 (1955) 51.